Science Translational Medicine
AAAS

www.sciencetranslationalmedicine.org/cgi/content/full/10/458/eaas9563/DC1

Supplementary Materials for

Thrombopoietin receptor–independent stimulation of hematopoietic stem cells by eltrombopag

Yun-Ruei Kao, Jiahao Chen, Swathi-Rao Narayanagari, Tihomira I. Todorova, Maria M. Aivalioti, Mariana Ferreira, Pedro M. Ramos, Celine Pallaud, Ioannis Mantzaris, Aditi Shastri, James B. Bussel, Amit Verma, Ulrich Steidl*, Britta Will*

*Corresponding author. Email: britta.will@einstein.yu.edu (B.W.); ulrich.steidl@einstein.yu.edu (U.S.)

Published 12 September 2018, *Sci. Transl. Med.* **10**, eaas9563 (2018)
DOI: 10.1126/scitranslmed.aas9563

The PDF file includes:

Other Supplementary Material for this manuscript includes the following:

(available at www.sciencetranslationalmedicine.org/cgi/content/full/10/458/eaas9563/DC1)

Table S7 (Microsoft Excel format). IPA analysis with DEGs in EP-treated mouse HSCs.
Table S8 (Microsoft Excel format). Altered metabolites detected in EP-treated HPC7 cells.
Table S9 (Microsoft Excel format). Pathway analysis with altered metabolites detected in EP-treated HPC7 cells.
Table S10 (Microsoft Excel format). IPA analysis with altered metabolites detected in EP-treated HPC7 cells.
Table S11 (Microsoft Excel format). Information on primary human-derived specimens.
Table S12 (Microsoft Excel format). List of antibodies used in FACS experiments.
Table S13 (Microsoft Excel format). List of primers for qPCR.

Supplementary Materials

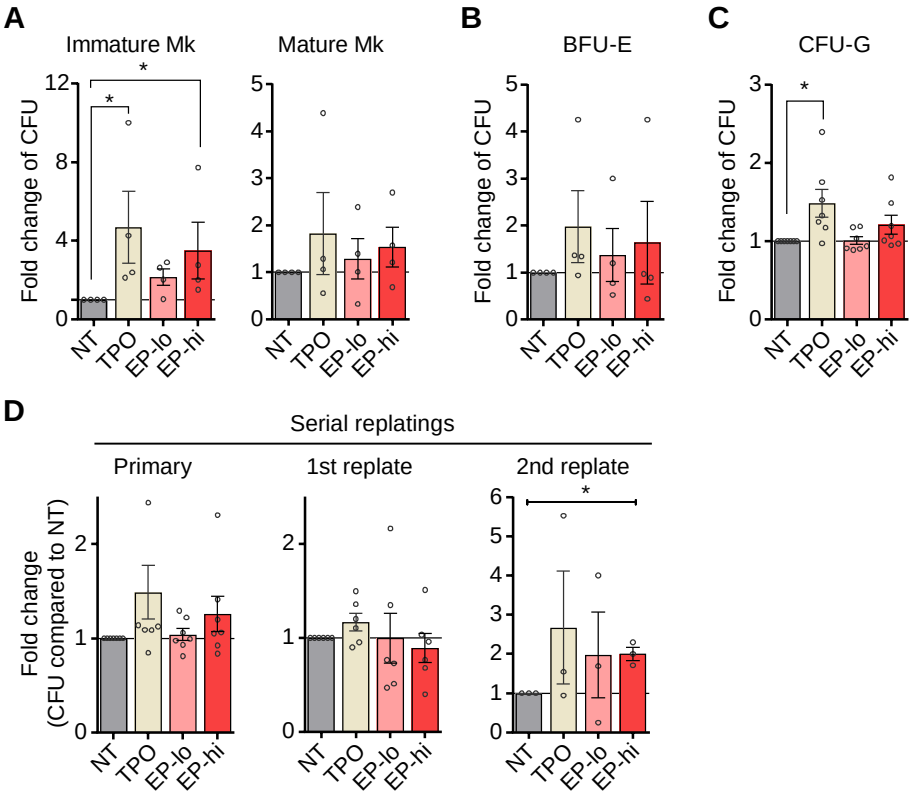

Fig. S1. Effects of EP on human MPP cells. (**A-B**) Megakaryocyte (**A**) and erythroid (**B**) colony formation in collagen-based culture system (n=4). (**C**) Granulocytic colony formation in methylcellulose semi-solid medium (n=7). CFU: colony-forming unit; MK: megakaryocyte colonies; BFU-E: erythroid colonies; CFU-G: granulocyte colonies. (**D**) Colonies from primary methylcellulose cultures were serially replated bi-weekly (n=7). Results are represented as fold change of colonies compared to non-treated (NT) vehicle control (H_2O). Data are mean ± SEM. *$p < 0.05$, **$p < 0.01$, ***$p < 0.001$(Paired Student's t-test).

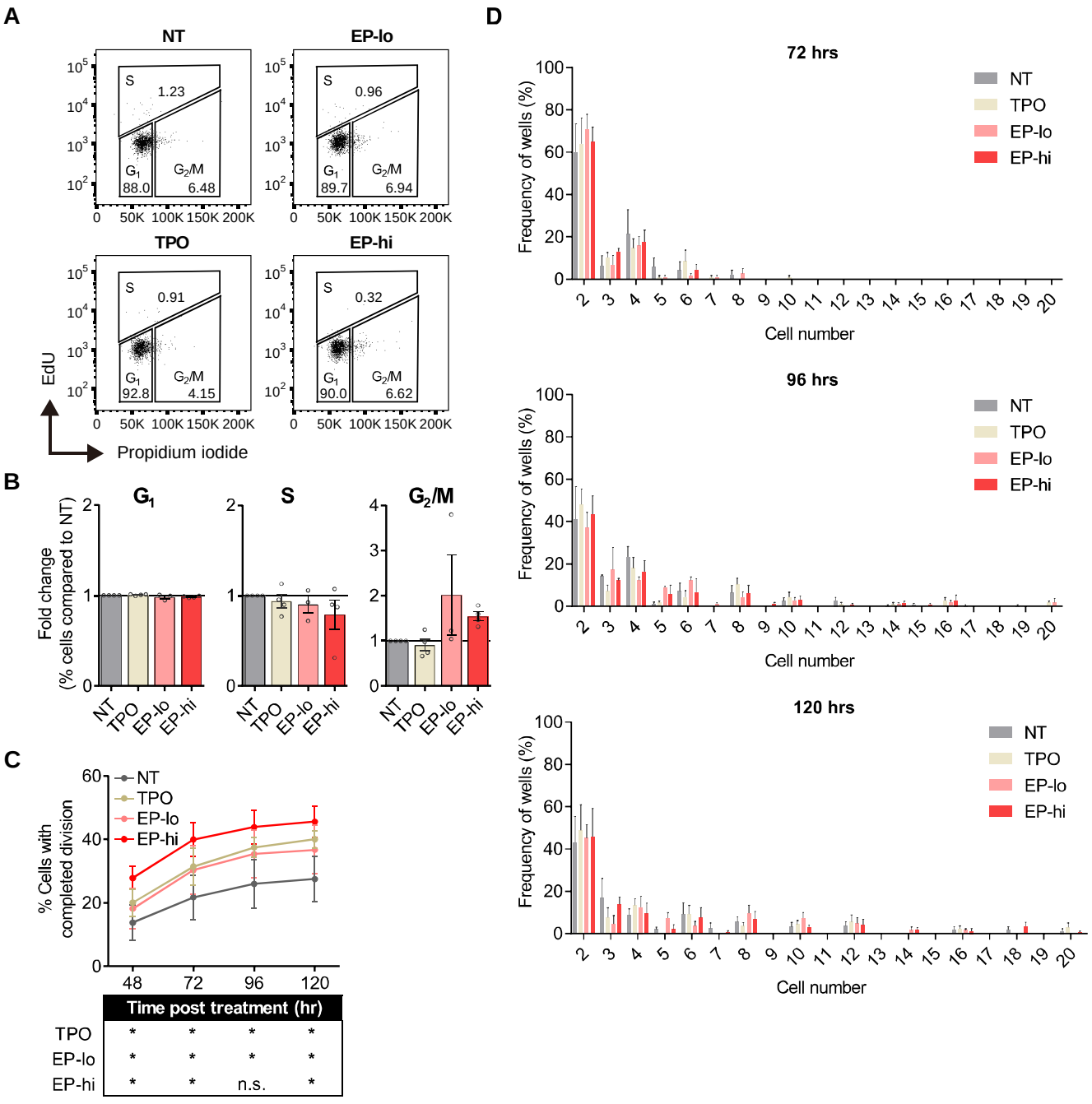

Fig. S2. Effects of EP on cell cycling of HSCs. (**A**) Representative FACS plots of EdU vs. propidium iodide (PI) in human HSCs after 24-hour treatment. (**B**) Fold change of % human HSCs in different stages of cell cycle (G_1, S, G_2/M) after 24-hour treatment compared to the vehicle control. G_1: EdU^-PI^-; S: EdU^+; G_2/M: EdU^-PI^+. (**C**) Fraction of HSCs with at least one completed division at different time points after treatment. Lower panel is showing the statistical significance compared to NT. Data are

mean ± SEM. n.s. non-significant. *$p < 0.05$ (Paired Student's t-test). (**D**) Frequency distribution of dividing cells per 120 single HSCs at 72, 96, and 120 hours after treatment. TPO: 100 ng/ml of recombinant human thrombopoietin, EP-lo: 3 μg/ml of eltrombopag, EP-hi: 10 μg/ml of eltrombopag.

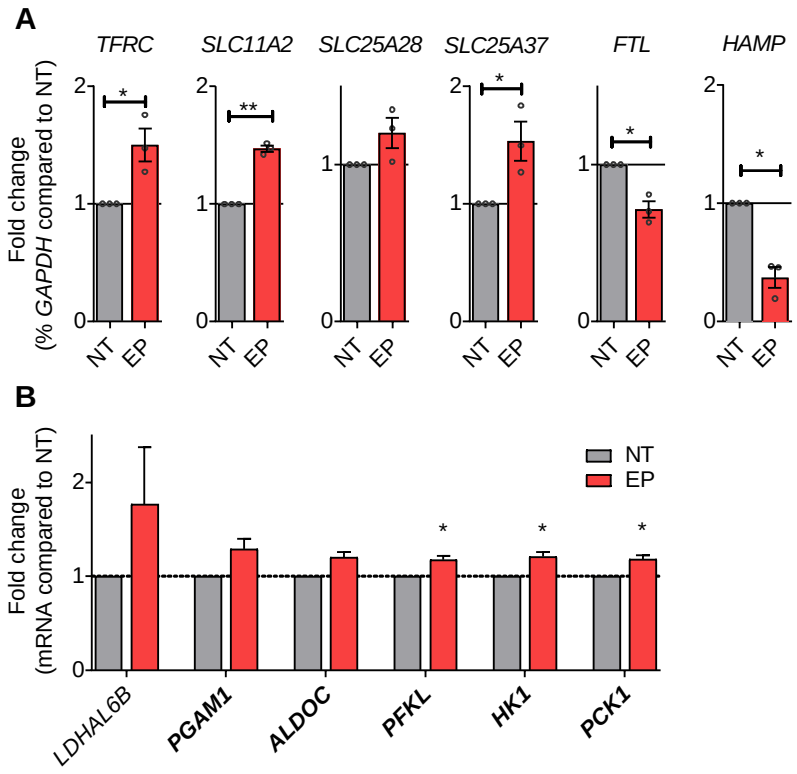

Fig. S3. Alterations of iron-associated gene expression in human hematopoietic cells after EP treatment. (**A**) Quantitative RT-PCR validation of iron-related genes in $CD34^-$ cells from healthy donors treated with either vehicle (H_2O) or EP (10 μg/ml) in liquid culture for 16 hours. Results are represented as fold change of % *GAPDH* compared to non-treated (NT) vehicle control (n=3). (**B**) Expression of glycolysis-related genes in the microarray analysis of human HSCs treated with either vehicle (H_2O) or EP (10 μg/ml) in liquid culture for 16 hours. Glycolysis-related genes that are also HIF1A targets are bold; n=4. All data represent mean ± SEM. *p < 0.05, **p < 0.01, ***p < 0.001 (Paired Student's t-test).

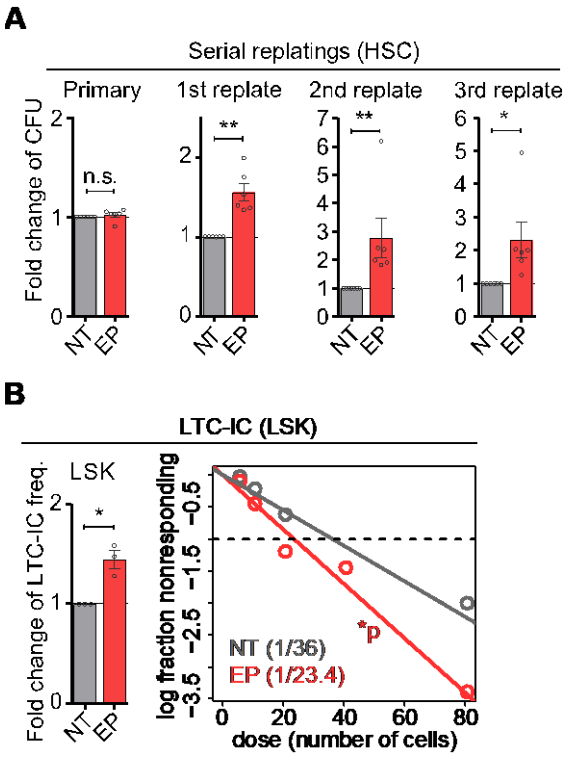

Fig. S4. TPO-R–independent stimulation of HSC self-renewal by EP. (**A**) Serial colony-forming capacity of c-*Mpl*$^{+/+}$ HSCs after EP treatment ex vivo. Results are expressed as fold change of colony-forming units compared to non-treated vehicle control (NT, n=6 independent experiments). (**B**) HSCs were enumerated by the LTC-IC assay using limiting dilutions of *Mpl*$^{+/+}$ LSK cells after ex vivo treatment with either vehicle control (NT, H_2O) or EP (10 μg/ml). Bar plot (left panel) showing LTC-IC frequency of individual mice expressed as fold change compared to NT (n=3 independent experiments). Scatter plot (right panel) showing LTC-IC frequency of EP (10 μg/ml) and NT (H_2O). The logged fraction of wells that did not form LTC-ICs (nonresponding) is plotted against limiting dilutions of LSK cells (n=3 independent experiments). LTC-IC frequency was determined using Poisson statistics and p-value was calculated using Chi-square on ELDA online server. All other data are mean ± SEM. *p < 0.05, **p < 0.01, n.s. (not significant) (Paired Student's t-test).

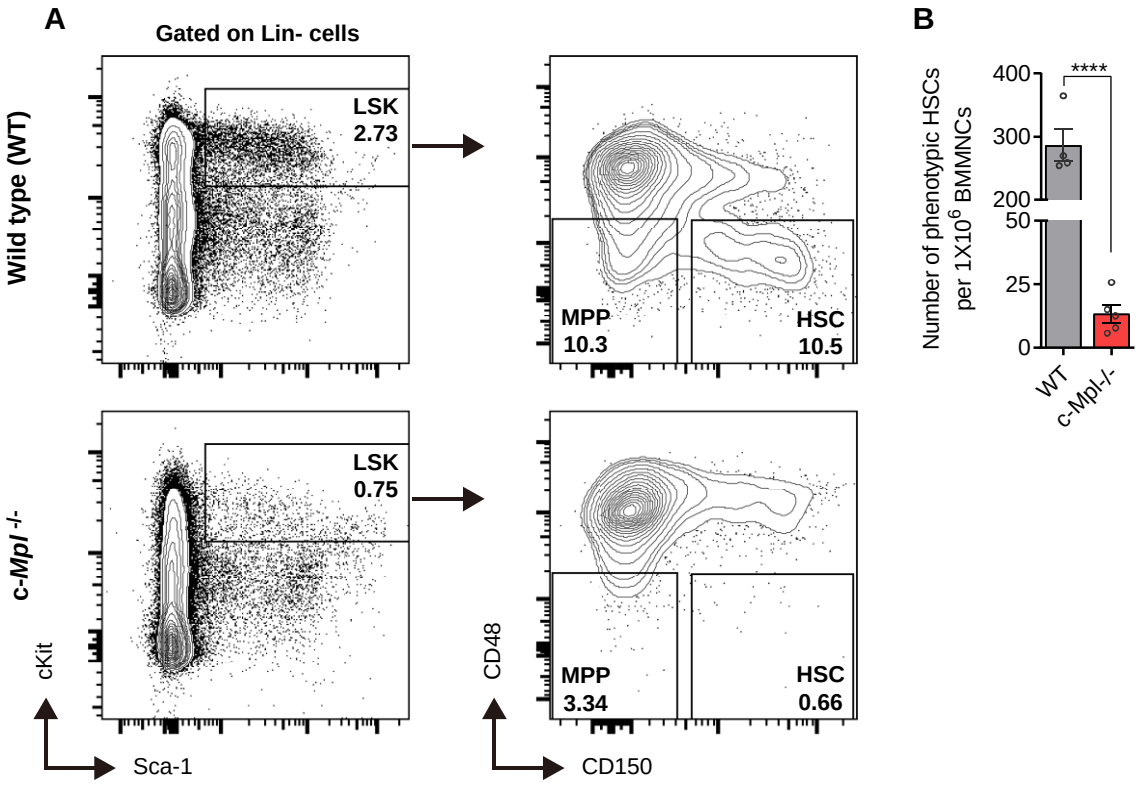

Fig. S5. Reduction of HSCs in c-Mpl$^{-/-}$ mice. (**A**) Cell surface expression of phenotypic HSCs ($Lin^{-}Sca\text{-}1^{+}c\text{-}Kit^{+}CD150^{+}CD48^{-}$) in wildtype (WT) and c-*Mpl*$^{-/-}$ mice. (**B**) Quantification of the number of phenotypic HSCs within 1x10^{6} bone marrow mononuclear cells (BMMNCs) in WT and c-*Mpl*$^{-/-}$ mice. n = 4 or 5. Data are mean ± SEM. ****p < 0.0001 (Unpaired Student's t-test).

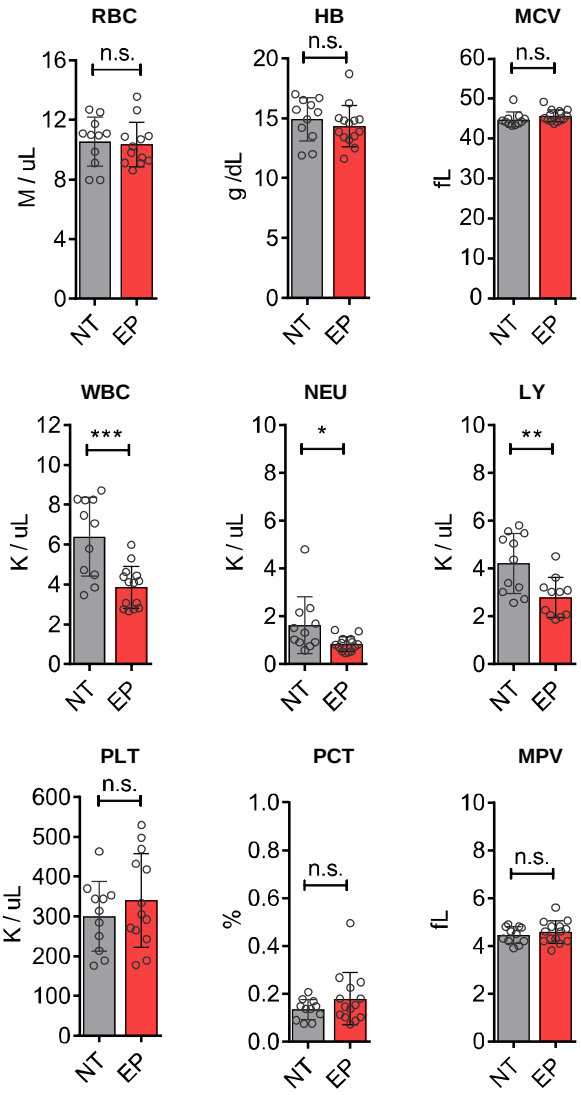

Fig. S6. Complete blood counts of c-Mpl$^{-/-}$ mice after in vivo treatment with EP. c-*Mpl*$^{-/-}$ mice were treated with EP (50 mg/kg) or vehicle control (H_2O) daily for 4 weeks by oral gavage. Complete blood count was performed using peripheral blood of the mice after 4-week treatment. RBC: red blood cells; HB: hemoglobin; MCV: mean corpuscular volume; WBC: white blood cells; NEU: neutrophils; LY: lymphocytes; PLT: platelets; PCT: plateletcrit; MPV: mean platelet volume. Data are mean ± SEM. ****p < 0.0001 (Unpaired Student's t-test).

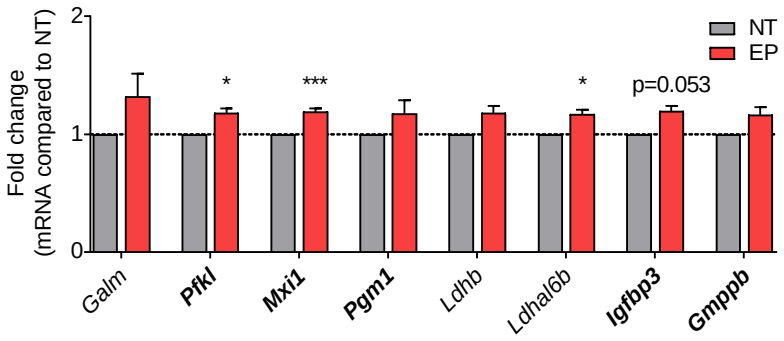

Fig. S7. Alterations of glycolysis-associated genes in mouse HSCs after EP treatment. Expression of glycolysis-related genes in mouse HSCs treated with either vehicle (H_2O) or EP (10 μg/ml) in liquid culture for 16 hours. Glycolytic genes that are also HIF1α targets are bold. Results are represented as fold change of % *Gapdh* compared to non-treated (NT) vehicle control. If not specified otherwise, data are mean ± SEM. **p* < 0.05, ***p* < 0.01, ****p* < 0.001 (Paired Student's t-test).

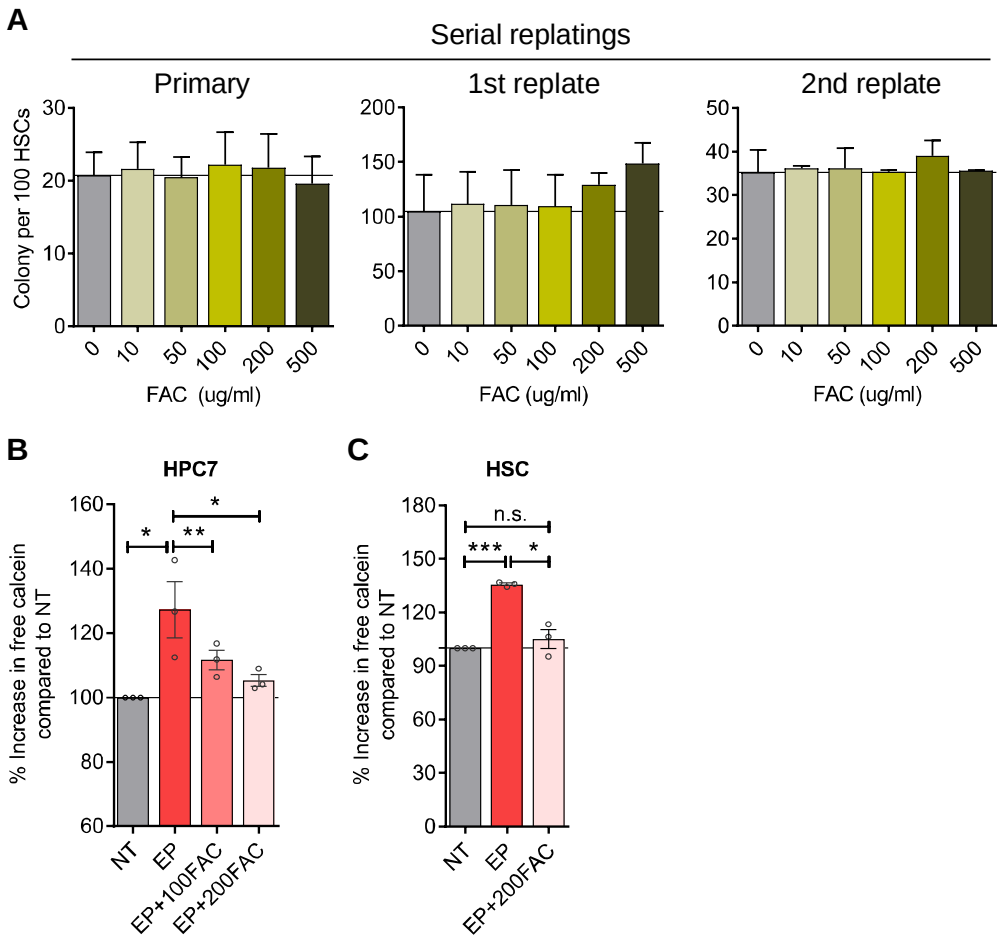

Fig. S8. FAC dose finding for ex vivo assays. (**A**) FACS-sorted mouse HSCs were preloaded with 0, 10, 50, 100, 200, or 500 μg/ml of ferric ammonium citrate (FAC) in liquid culture for 1 hour before being subjected to methylcellulose colony-forming assay. Results are represented as fold change of colonies compared to vehicle control (NT, 0 μg/ml of FAC). Colonies from the primary plating were harvested and preloaded with increasing concentrations of FAC for an hour before being subjected to subsequent serial replating in the colony-forming assay (n = 4). (**B, C**) Calcein staining to measure the concentration of intracellular iron in HPC7 cell line (**B**) or HSCs (**C**). Results are presented as mean fluorescence intensity of calcein in HSCs in different treatment conditions relative to the vehicle control (H_2O, NT). If not specified otherwise, data are mean ± SEM. **p* < 0.05, ***p* < 0.01, ****p* < 0.001 (Paired Student's t-test).

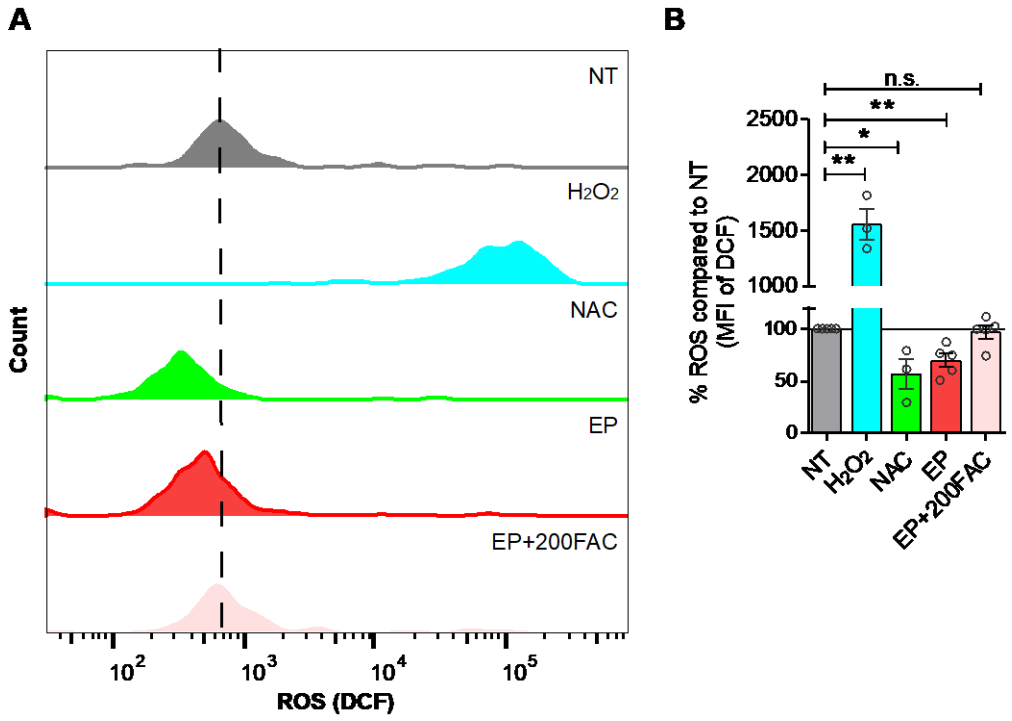

Fig. S9. Intracellular ROS concentrations in HSCs after EP treatment. (**A**) Representative histograms showing mean fluorescence intensity (MFI) of DCF, which directly measures intracellular ROS in mouse BMMNCs treated with vehicle control (NT), positive control (H_2O_2), negative control (NAC, N-acetyl cysteine), or EP with (EP+200FAC) or without rescue. Cells were subsequently stained with stem and progenitor cell markers (Lin-Sca1+cKit+CD150+CD48-CD34-) to quantify ROS specifically in the HSC compartment. (**B**) Quantification of MFI of DCF in the HSC compartment after treatment. Mouse BMMNCs were incubated with 0 or 200 μg/ml of FAC for 1 hour at 37ºC before being subjected to treatment in liquid culture for 1 hour. H_2O_2 : 200 μM, NAC: 5 mM, EP: 10 μg/ml of eltrombopag, 200FAC: 200 μg/ml of ferric ammonium citrate. n = 3-5. Data are mean ± SEM. *$p < 0.05$, **$p < 0.01$, ***$p < 0.001$ (Paired Student's t-test).

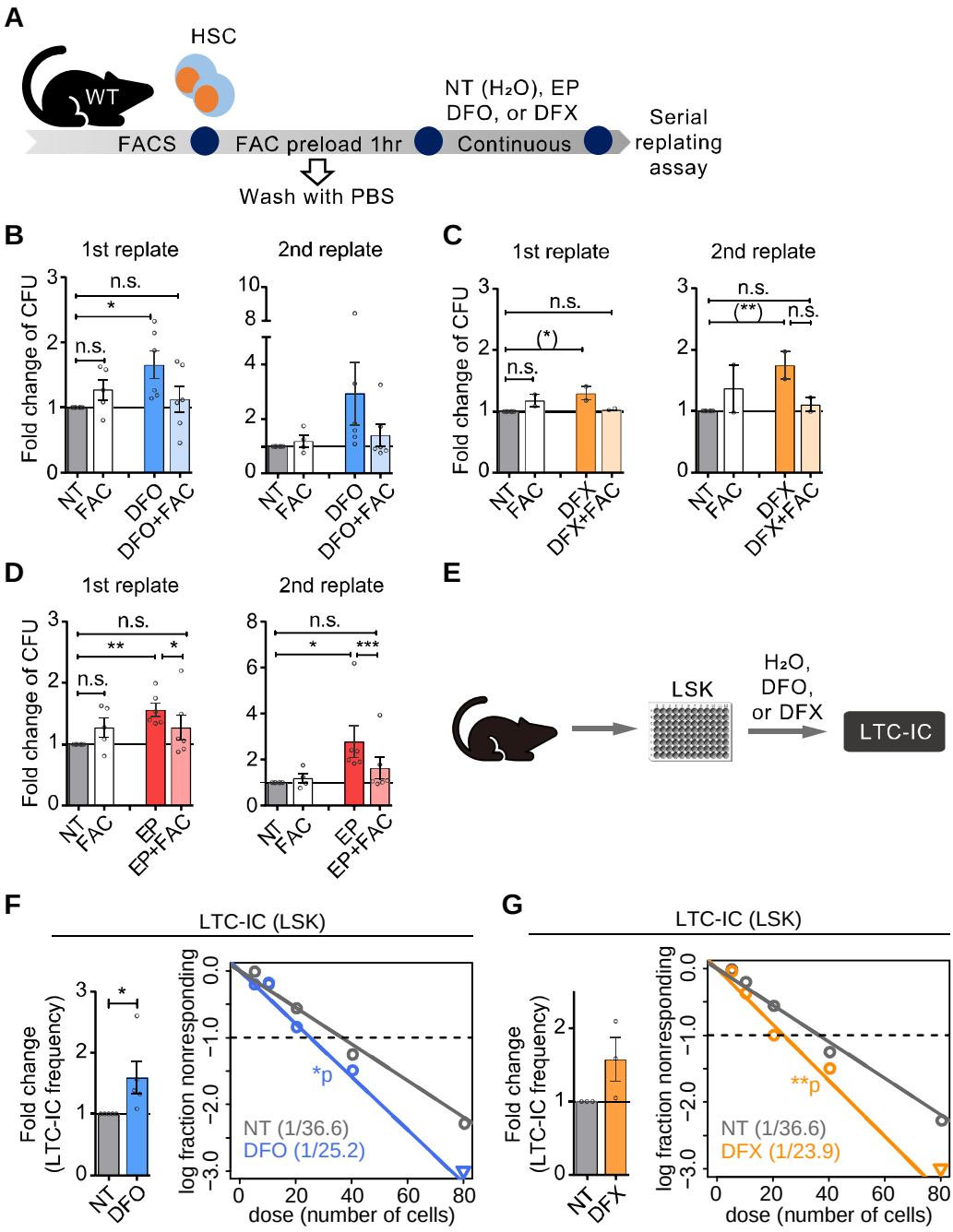

Fig. S10. Iron-dependent HSC self-renewal upon chelator treatment. (**A**) Scheme showing HSCs isolated from wildtype mice preloaded with 200 μg/ml of FAC for 1 hour before iron chelator treatment, to examine the effects of iron chelation on HSCs. (**B-D**) Serial colony-forming capacity of HSCs upon treatment with DFO (**B**, n=6), DFX (**C**, n=2), or EP (**D**, n=5), rescued with FAC. (**E**) Scheme showing ex

vivo treatment with DFO or DFX and functional assessment of HSC frequency in wildtype mice. LSK cells were sorted directly into 96-well plates and treated with DFO (10 μM), DFX (5 μM), or vehicle control (0.01% DMSO) in LTC-IC assay. (**F, G**) HSC frequency in LSK cells enumerated by the LTC-IC assay. Left panel: LTC-IC frequency in each individual donor (n=4). Right panel: scatter plot showing LTC-IC frequency of LSK cells in NT, DFO-treated (**F**, n=5), or DFX-treated groups (**G**, n=3). HSC frequencies were determined using Poisson statistics and p-value was calculated using Chi-square on ELDA online server. If not specified otherwise, data are mean ± SEM. **p* < 0.05, ***p* < 0.01, ****p* < 0.001 (Paired Student's t-test).

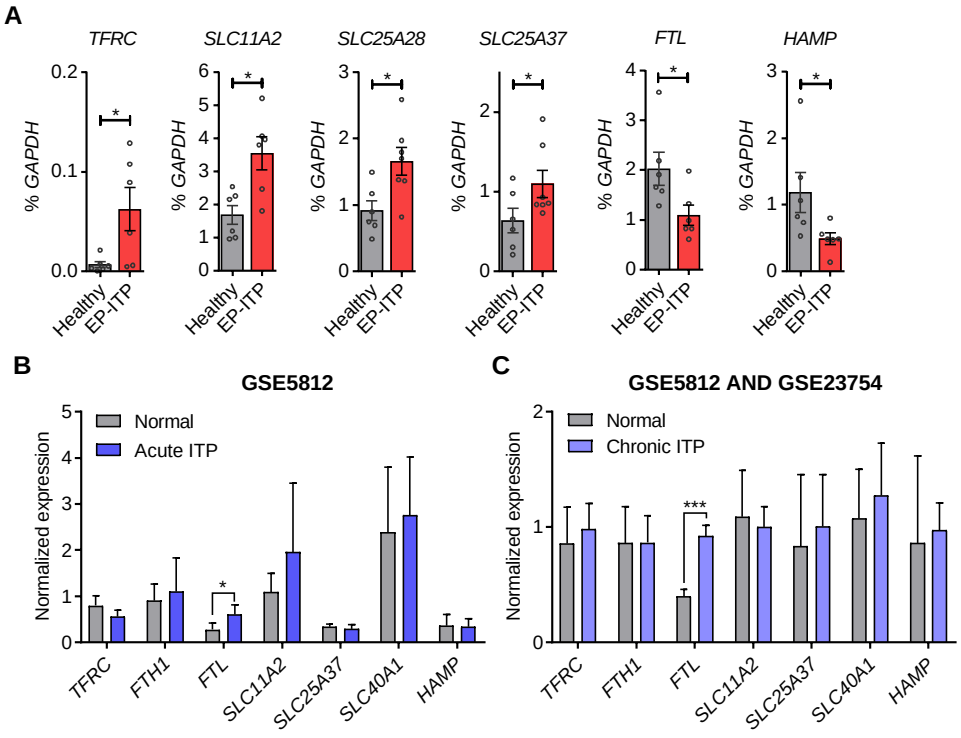

Fig. S11. Iron-associated gene expression changes in ITP patients treated with EP. (**A**) Quantitative RT-PCR validation of iron-related genes in $CD34^-$ cells from ITP patients treated in vivo with EP compared to healthy donors. (**B**, **C**) Expression of iron-related genes in primary patients with acute ITP (**B**) or chronic ITP (**C**) compared to healthy individuals. We reanalyzed gene expression datasets from GEO database with the accession numbers GSE5812 and GSE23754. The normalized expression values of iron-related genes are shown. If not specified otherwise, data are mean ± SEM. *$p < 0.05$, **$p < 0.01$, ***$p < 0.001$ (Unpaired Student's t-test).